2014

Activation of autophagy and AMPK by gamma-tocotrienol suppresses the adipogenesis in human adipose derived stem cells

Lu Zhao
University of Florida

Jung-Heun Ha
University of Florida

Meshail Okla
University of Florida

Soonkyu Chung
University of Nebraska-Lincoln, schung4@unl.edu

Published in *Molecular Nutrition & Food Res.* 58 (2014), pp. 569–579. doi 10.1002/mnfr.201300157

Submitted February 28, 2013; revised July 24, 2013; accepted: August 3, 2013.
Supporting information follows the References.

PMID: 24668775

Activation of autophagy and AMPK by gamma-tocotrienol suppresses the adipogenesis in human adipose derived stem cells

Lu Zhao, Jung-Heun Ha, Meshail Okla and Soonkyu Chung

Department of Food Science and Human Nutrition, University of Florida, Gainesville, FL, USA

Corresponding author — Dr. Soonkyu Chung, Department of Nutrition & Health Sciences, University of Nebraska–Lincoln, 316G LEV, Lincoln, NE 68583-0806, USA; email schung4@unl.edu

Abstract

Scope: This study investigated the mechanistic details by which gamma-tocotrienol (γ-T3) manipulates adipocyte differentiation in human adipose derived stem cells (*h*ASCs).

Methods and results: γ-T3 specifically inhibited the early stage of adipocyte differentiation by acting on downstream of C/EBP-β but upstream of C/EBP-α in *h*ASCs. In searching a potential mechanism, we identified that γ-T3 promoted two catabolic signaling pathways: (i) AMP kinase (AMPK), and (ii) enhanced autophagy, as assessed by autophagic flux and cytosolic autophagosome (LC3II) accumulation. In addition, chronic exposure of γ-T3 induced caspase3-mediated apoptotic cell death. The blockage of AMPK by a dominant negative mutant of AMPK was insufficient to normalize γ-T3-mediated autophagy, suggesting that enhanced autophagic activity of γ-T3 is independent of AMPK activation. Intriguingly, AMPK inhibition significantly restored PPAR-γ activation, but marginally rescued lipid-loaded adipocyte morphology due to, at least partly, a lack of lipid droplet-coating protein. These data suggest that γ-T3 activates AMPK and autophagy signaling, which synergistically contributes to the suppression of adipogenic conversion of *h*ASCs into adipocytes.

Conclusion: These results provide a novel insight into the molecular mechanism involved in anti-adipogenic action of γ-T3 in humans via AMPK and autophagy activation. Thus, γ-T3may constitute a new dietary avenue to attenuate hyperplastic obesity in humans.

Keywords: Adipogenesis, AMP kinase, Autophagy, Gamma-tocotrienol, Obesity

Abbreviations: Ad, adenovirus; **AMPK**, AMP kinase; **C/EBP**, CCAAT/enhancer-binding proteins; **CQ**, chloroquine; **DN**, dominant negative; *γ*-T3, gamma-tocotrienol; **GFP**, green florescent protein; ***h*ASCs**, human adipose derived stem cells; **mTOR**, mammalian targets of rapamycin; **PPAR-*γ***, peroxisome proliferator activated receptor gamma; **PLIN**, perilipin; **T3s**, tocotrienols; **TPs**, tocopherols

1 Introduction

Vitamin E is a generic descriptor that includes derivatives of tocopherols (TPs) and tocotrienols (T3s). Due to an unsaturated isoprenoid side chain, T3s are smaller, more hydrophobic, and thus more proficient for penetration into cell membrane than TPs. T3s are further categorized into alpha, beta, gamma, and delta isoforms depending on the substitution pattern of methyl groups on the chromanol ring. Among these isomers, gamma-tocotrienol (*γ*-T3) displays multiple bioactivities including lowering cholesterol synthesis and cardiovascular risk [1–3], attenuating hepatic TG accumulation [4–6], improving insulin sensitivity [7, 8], and reducing the risk of cancer [9–12] in cells, animal models, and some human studies. These immune-modulatory and antiproliferative characteristics of *γ*-T3 are attributed to its ability to modify pathological conditions by targeting multiple pathways (review in [13]), including NFκB [14, 15], Wnt [16], mammalian targets of rapamycin (mTOR) [11, 17], and autophagy [9, 18, 19]. Despite a large body of evidence that *γ*-T3 is an extraordinary signaling modifier in various cell types, only limited information is available as to whether *γ*-T3 modifies the signaling pathways in adipocytes.

More than 16 percent of children and adolescents are obese in the United States, and the prevalence has more than tripled over the past three decades [20, 21]. One of the prominent pathophysiological features of childhood obesity is adipogenesis, an increase in the number of fat cells resulting from the conversion of mesenchymal stem cells into new adipocytes (also known to adipocyte hyperplasia). Prevention of childhood obesity is critical, as the abnormal hyperplasia in childhood predisposes to a higher risk of metabolic complications in adulthood including type 2 diabetes and cardiovascular diseases [22]. Adipogenesis is under the control of a cascade of transcription factors including CCAAT/enhancer binding proteins (C/EBPs) and peroxisome proliferator activated receptor gamma (PPAR-*γ*); it is well established that terminal adipocyte differentiation is driven by the master transcription factor PPAR-*γ*. However, the molecular dynamics of early-phase adipogenesis remains to be unraveled. Studies in cultured cells and in animals have shown that a disturbance of signaling pathways frequently modified in cancer could also affect adipogenesis. For example, inhibition of histone deacetylase activity [23], activation of wingless signaling [24], limited

nutrient availability or energy homeostasis [25], and interruption of autophagy [26, 27] have all been negatively correlated with white fat cell formation. In support of this concept, several phytochemicals, which are not PPAR-γ antagonists per se, have been shown to exert anti-adipogenic activity by targeting the aforementioned signaling pathways [28–30]. Moreover, inhibition of adipogenesis is often accompanied by apoptosis [31, 32], suggesting that early-phase adipogenesis is also the critical step for determining cell fate.

Much mechanistic information on adipogenesis is derived from 3T3L1 preadipocytes, a well-established murine hybridoma cell line. Previously, Uto-Kondo et al. reported that γ-T3 inhibits the conversion of 3T3L1 preadipocytes into adipocytes via modification of Akt signaling [33]. Our rationale for using human adipose derived stem cells (*h*ASCs) was based on the following reasons: (i) 3T3L1 preadipocytes are mouse hybridoma cells, thus it is difficult to distinguish anti-adipogenic effects from antitumor effects; (ii) 3T3L1 preadipocytes are committed preadipocytes that have already lost their stem cells properties; and (iii) 3T3L1 preadipocytes undergo postconfluent mitogenic expansion, which is not found in primary adipogenic precursor cells [34]. Therefore, investigation of anti-adipogenic mechanism of γ-T3 in the unmodified human adipocyte precursor cells would be important to attain physiological significance. Here, we report that γ-T3 is a potent negative regulator of adipogenesis in *h*ASCs by manipulating catabolic signaling pathways including AMP kinase (AMPK)/mTOR and the autophagy/apoptosis axis, which have not been reported previously in 3T3L1 cells.

2 Materials and methods

2.1 Chemicals reagents

All cell culture wares were purchased from Fisher Scientific. Fetal bovine serum and penicillin-streptomycin were purchased from Cellgro Mediatech, Inc. (Herndon, VA, USA). Rosiglitazone (BRL49653) was purchased from Cayman Chemical. All other chemicals and reagents were purchased from Sigma Chemical Co (St. Louis, MO, USA), unless otherwise stated.

2.2 Preparation of *h*ASCs and adipogenic differentiation

Abdominal adipose tissue was obtained from females with a body mass index of ~30 during liposuction or abdominal plastic surgeries. All protocols and procedures were approved by the Institutional Review Board (#693–2011) at the University of Florida. Isolation of *h*ASCs and differentiation of into adipocytes were conducted as Skurk et al. described previously [35]. Briefly, tissue was minced and enzymatically digested for 45 min in a

Krebs-Ringer buffer containing 1 mg/mL collagenase (CLS-1; Worthington) and 2% BSA. The digested tissue was then filtered through 100 μm mesh and pelleted by centrifuging at 600 × *g* for 5 min. The collected *h*ASCs were resuspended in red blood cell lysis buffer (Biolegend) for 10 min and centrifuged to remove most of the contaminating erythrocytes. Cultures of *h*ASCs were grown in proliferation medium containing DMEM/Ham's F12, 10% fetal bovine serum, 15 mM HEPES (pH 7.4), 50 U/mL penicillin and 50 μg/mL streptomycin. For induction to adipogenic differentiation, cells were seeded ($5 \times 10^5/cm^2$) in 6-well dishes and allowed to attach for 24 h in proliferation medium. After attachment, cultures were grown for the next 3 days in differentiation medium containing 0.25 mM isobutylmethylxanthine, 1 μM rosiglitazone, and 500 nM human insulin in commercially available human adipocyte medium (AM-1, ZenBio). Adipocyte medium (AM-1) was replenished every 3 days. Under these conditions, approximately 50–80% of the cells differentiated into adipocytes by 10–12 days post differentiation. Each independent experiment was repeated at least twice using a mixture of cells from three or four subjects to avoid individual variation.

2.3 Preparation of T3s and TP

Isomers of α-, β-, and *γ*-T3s with a purity of 70, 60, and 90%, respectively, were kindly provided by Carotech Inc. (Edison, NJ). α-TP was purchased from Sigma. Five millimolar of T3s (α-, β-, and *γ*-T3) and TP were prepared in DMSO as Ahn et al. described previously [14]. Small aliquots of T3s and TP stock were kept at −20 °C and freshly diluted to 0.1–10 mM at the time of addition to *h*ASCs.

2.4 Cell viability assay

The cytotoxic effect of T3s was determined using the XTT cell viability kit (Cell Signaling Technology) according to the manufacturer's protocol. Briefly, undifferentiated and fully differentiated *h*ASCs were cultured in 96-well plates with a seeding density of ~20 000 cells/well. Cells were incubated with either DMSO or increasing concentrations of T3 isomers for 24 h (Fig. 1). Medium was then replaced with fresh medium containing XTT solution for 3 h at 37°C before measurement of OD 450 nm using a Synergy H1 hybrid plate reader (BioTek).

2.5 qPCR and microarray analysis

Gene-specific primers for real-time quantitative PCR (qPCR) were obtained from Integrated DNA Technologies (Chicago, IL,USA). Total RNA was isolated with Trizol reagent (Invitrogen). To remove the potential genomic DNA

contamination, mRNA was treated with DNase (Mediatech), and 2 μg of mRNA was converted into cDNA in a total volume of 20 μL (iScript cDNA synthesis kit, Bio-Rad). Gene expression was determined by real-time qPCR (CFX96, Bio-Rad), and relative gene expression was normalized by the average of two reference genes, 36B4 and GAPDH (primer sequences are available in Supporting Information Table 1).

2.6 Western blot analysis

To prepare total cell lysates, monolayers of *h*ASC cultures were scraped with ice-cold radioimmune precipitation assay buffer (Thermo Scientific) with protease inhibitors (Sigma) and phosphatase inhibitors (2 mM Na_3VO_4, 20 mM β-glycerophosphate, and 10 mM NaF). Proteins were fractionated using 8 or 10% SDS-PAGE, transferred to PVDF membranes, and incubated with the relevant antibodies. Chemiluminescence from ECL (Western Lightning) solution was detected with FluorChem E (Cell Biosciences). For the detection of LC3 I and II bands, 15% SDSPAGE was used and the proteins were transferred to a PVDF membrane with a semidry transfer unit (Hoefer TE77X). Polyclonal or rabbit monoclonal antibodies targeting phospho-Akt (Ser473, #4060), total Akt (#9279), phospho-extracellular signal-related kinase (ERK) (#4370), total-ERK (#4695), phospho-mTOR (#5536), total mTOR (#2983), phospho-p70S6 kinase (#9280), total p70S6 kinase (#2708), phospho-AMPK (#2535), total-AMPK (#2630), cleaved PARP (#5625), cleaved caspase-3 (#9664), PPAR-γ (#2443), FAS (#3180), β-actin (#4967), LC3 (#9562), p62 (#8025), beclin-1 (#3738), and IκBα (#4812) were purchased from Cell Signaling Technology. The mouse monoclonal antibodies for aP2 were purchased from Santa Cruz Biotechnology.

2.7 Adenoviral delivery of dominant negative AMPK and LC3-GFP

Adenovirus (Ad) harboring null AMPK α mutation (dominant negative, Ad AMPK-DN) was a generous gift from Dr. Jae Bum Kim at Seoul National University. Green florescent protein (GFP)-tagged Ad LC3 was a gift from Jae-Sung Kim at the University of Florida [36, 37]. Ad AMPK-DN, Ad LC3-GFP, and Ad GFP were amplified as previously described by Lee et al. [38]. The titration of recombinant Ad was performed using a commercial titration kit (Adeno-XTM Rapid Titer kit, Clonetech). To determine the autophagy activation, either Ad GFP or Ad LC3-GFP were infected (MOI 5) in *h*ASCs before adipogenic differentiation (Fig. 5). To determine whether inhibition of AMPK activity rescues *h*ASCs from γ-T3-mediated suppression of adipogenesis, Ad-AMPK-DN or Ad-GFP (MOI 5) was delivered 24 h before adipogenic stimulation followed by γ-T3 (1 μM) stimulation for 7 days (Fig. 6).

2.8 Immunofluorescence

*h*ASCs were cultured on coverslips for immunofluorescence microscopy and stained as described previously [39]. Briefly, cells were fixed with 3.7% paraformaldehyde in PBS for 20 min, and then the coverslips were blocked and permeabilized with 0.1% saponin, 10 mM glycine, and 1.25 mg/mL goat serum for 1 h. For immuno-fluorescent staining of LC3 (Fig. 5D), the cover slips were incubated with a 1:25 dilution of the LC3B antibody (Cell signaling) overnight at 4°C, followed by incubation with a 1:300 dilution of rhodamine red-conjugated goat antirabbit IgG (Jackson Immunoresearch) for 1 h. Florescent images were captured using a digital inverted fluorescence EVOS microscope (AMG). 4′,6-diamidino-2-phenylindole (DAPI) staining (1 μg/mL) was used for counter staining of the nucleus. Additionally, fragmented nuclei (due to chronic *γ*-T3 treatment) were also visualized by DAPI staining (Fig. 5E).

2.9 Statistical analysis

Results are presented as means ± SEM. The data were statistically analyzed using Student's *t*-test or one-way ANOVA with Tukey's multiple comparison test. All analyses were performed with GraphPad Prism 5 (Version 5.04).

3 Results

3.1 *γ*-T3 specifically inhibits the early stage of adipocyte differentiation

It has been shown that *γ*-T3 induces apoptosis in malignant tumor cells but not in mitogenically quiescent cells [12]. However, it is unknown whether *γ*-T3 affects the cell viability of human mesenchymal stem cells. To address this question, increasing doses (0.1–10 μM) of α-, β-, *γ*-T3, and α-TP were incubated with either undifferentiated *h*ASCs (Fig. 1A), or fully differentiated human mature adipocytes (Fig. 1B) in comparison to vehicle control (DMSO). As we expected, TP and α-T3 had no significant cytotoxic effects compared to the control. In contrast, an exposure to a high dose of *γ*-T3 or δ-T3 reduced cell viability in both the *h*ASC cultures (>1 _M) and in mature adipocytes (>5 μM) (Fig. 1).

It has been shown that T3, but not TP, suppressed adipogenic differentiation in 3T3L1 cells, a well-studied murine preadipocyte cell line [33]. To determine whether T3 was able to inhibit adipogenesis in uncommitted cells, *h*ASCs were induced to differentiate into adipocytes with either T3 isomers or TP for 10 days at different doses (0.1, 0.5, and 1 μM) compared to DMSO

(vehicle) control (Fig. 2A). Consistent with a previous report in 3T3L1 cells, only T3s-inhibited adipogenesis in *h*ASCs; TP did not show any significant impact on TG accumulation and adipogenic gene expression (Supporting Information Fig. 1). The rank order of anti-adipogenic potential was *γ*-T3 > *δ*-T3 >> *α*-T3 as assessed by triglyceride accumulation using Oil-red O staining. Intriguingly, this anti-adipogenic effect was selective in the early stage of differentiation (d1–d4). When T3s were added on day 4, the anti-adipogenic effect of T3s was abolished (Fig. 2B). Similarly, when T3s were added to fully differentiated cells on day 10, *γ*-T3 and δ-T3 did not seem to impose any anti-adipogenic or antilipogenic effects, showing no changes of adiposity or any signs of dedifferentiation (Fig. 2C). These results show that the anti-adipogenic effects of T3 in *h*ASCs are isomer-specific and time-sensitive, only effective in the early stage of adipogenesis.

To further confirm the anti-adipogenic effects of T3s, the *h*ASCs were first induced to differentiate with either T3 isomer or TP treatment, and then adipogenic gene expression levels were quantified by qPCR. The adipocyte marker gene expression was extremely reduced in cultures treated with T3, especially with *γ*-T3 and δ-T3, and to a lesser extent with α-T3 (anti-adipogenic potency *γ*-T3 > *δ*-T3 >> *α*-T3); the master adipogenic transcription factors of C/EBP-α and PPAR-*γ* were dramatically reduced in cultures with *γ*-T3 and δ-T3, without any change occurring in the C/EBP-β expression level. Downstream target genes of PPAR-*γ*, including fatty acid binding protein 4 (FABP4, also known as aP2), adiponectin, hormone-sensitive lipase, glucose transporter 4, and the lipid droplet-coating protein perilipin (PLIN), were all significantly reduced correspondingly. Notably, there was no significant increase in the expression of inflammatory gene TNF-α; this supports that the inhibition of adipogenesis by *γ*-T3 was not accompanied by inflammation (Fig. 3A). We next profiled the expression of C/EBP genes during the first 48 h of adipogenesis. *γ*-T3 treatment failed to trigger C/EBP-α at 48 h without any significant difference in C/EBP-δ and C/EBP-β profiles, suggesting that *γ*-T3 acts on upstream of C/EBP-α but downstream of C/EBP-β to control adipogenesis (Fig. 3B). In parallel, the extent to which *γ*-T3 and δ-T3 reduced the adipogenic protein expression levels of PPAR-*γ*, aP2, and fatty acid synthase were equivalent to their attenuation in the adipogenic gene profile (Fig. 3C). Based on these results, we determined that a 1 μM dose of *γ*-T3 was potent to inhibit new fat cell formation of *h*ASCs. Thus, 1 μM *γ*-T3 was used for the remainder of the studies to further investigate the anti-adipogenic mechanism of *γ*-T3.

3.2 *γ*-T3 alters Akt/mTOR/AMPK pathway

It has been previously reported that *γ*-T3 attenuates adipogenesis in 3T3L1 preadipocytes through Akt signaling modification [33]. To verify whether

the delayed insulin response is also the mechanism responsible for reduced adipogenesis in *h*ASCs, we examined the basal- and insulin-stimulated responses. There was no significant difference in insulin-stimulated Akt and ERK phosphorylation (Fig. 4A). Although basal Akt phosphorylation seemed to be reduced (~30%) in γ-T3-treated cultures compared to control (Fig. 4C), the insulin responsive machinery seems to be intact in *h*ASCs in the presence of γ-T3.

Several phytochemicals are known to inhibit adipogenesis through the mechanism related to AMPK activation [29, 30, 38]. AMPK is regarded as a major energy-sensing regulator that activates a variety of catabolic processes and simultaneously prevents anabolic processes via inhibition of the mTOR pathway [40]. To investigate whether γ-T3 is able to modify energy- and nutrient-sensing pathways, we examined AMPK and mTOR signaling. Treatment with γ-T3 decreased mTOR phosphorylation and its downstream target p70S6 kinase compared to TP treatment (Fig. 4B) or vehicle control (Fig. 4C). A decrease of mTOR and Akt phosphorylation was concurrent with an increase of AMPK phosphorylation (Fig. 4C), indicating that catabolic signals are upregulated with γ-T3 treatment.

3.3 γ-T3 increases chronic autophagy and promotes apoptotic cell death

Autophagy, a self-digestive process, is an essential signaling pathway for white adipocyte differentiation [41]. Autophagy is also a principal pathway that determines cell fate in response to stress by adjusting energy requirements such as starvation [42]; under glucose starvation, autophagy is promoted by AMPK to generate nutrients and maintain energy homeostasis, while autophagy is inhibited by mTOR activation, a integrative growth signal [43–45]. Because we observed that γ-T3 alters nutrient sensing signals (a decrease of p-mTOR but an increase of p-AMPK, Fig. 4),we hypothesized that γ-T3 will promote autophagic degradation, which will be distinct from the constitutive autophagy for white fat cell differentiation. To address this question, we first investigated the dynamics of autophagy in *h*ASCs during adipogenic differentiation. As we expected, insoluble autophagosome formation (LC3II bands) increased robustly starting at the exit of the early differentiation stage (d4); additionally, the levels remained higher after terminal differentiation compared to undifferentiated *h*ASCs. The increase of autophagy during adipocyte differentiation was parallel to (i) an increase of beclin 1 (Atg6), a critical component for nucleation of autophagic vesicles; (ii) an degradation of p62/SQSTM1, an adapter protein that is selectively degraded via autophagy; and (iii) an increase of adipogenic markers of PPAR-γ and aP2 (Fig. 5A). Furthermore, addition of chloroquine (CQ), an inhibitor of lysosomal degradation, increased LC3II accumulation, confirming

the augmented autophagy flux during adipogenic differentiation (data not shown). Interestingly, despite the reduced adipogenesis (low expression of aP2), γ-T3 treatment enhanced autophagosome formation (increase of insoluble LC3II) as well as p62 degradation (Fig. 5B). Noticeably, an increase of autophagy by γ-T3 was not coupled to an increase of beclin-1 (Fig. 5B), suggesting that γ-T3 treatment may trigger a beclin 1-independent autophagic degradation in comparison to the obligatory autophagy for adipocyte differentiation seems to be beclin 1-dependent. An increase of autophagy flux by γ-T3 was also confirmed by immunostaining of LC3 in the presence of CQ as well as the adenoviral delivery of GFP-tagged LC3 (in the absence of CQ); accumulation of autophagosome (LC3II) in cytoplasm was increased in cultures with γ-T3 treatment compared to TP control (Fig. 5C).

It has been shown that autophagy and apoptosis are intimately involved in deciding cell fate (survival versus cell death), and usually these two processes are mutually exclusive of each other [46]. Hence, we next asked whether γ-T3 causes autophagic cell death instead of apoptotic cell death. After chronic exposure of γ-T3 for 10 days, cleaved PARP and caspase-3 peptide were detectable by Western blot analysis, showing that cells are eventually undergoing caspase 3 dependent apoptotic cell death (Fig. 5D). Apoptotic cell death was also confirmed in fragmented-nuclei by DAPI staining (Fig. 5E). The Bax/Bcl-2 ratio, a determinant for apoptosis, was dramatically increased (~20 fold) at day 10 (Fig. 5F). This increase was mostly due to a compromised Bcl-2 gene expression rather than an increase of Bax, implicating that decreased Bcl-2 levels may be a metabolic switch from progressive autophagy to apoptosis. Thus, these findings reveal that γ-T3 causes aberrant autophagy during adipocyte differentiation, which eventually induces caspase 3-mediated cell death in *h*ASCs.

3.4 Inhibition of AMPK activation partially restores PPAR-γ expression but not autophagy activation

To further determine whether inhibition of AMPK activation could reverse the anti-adipogenic effects of γ-T3, we used a dominant negative strategy by delivering a kinase-null mutant of AMPK (Ad AMPK-DN). *h*ASCs were infected with either Ad GFP or Ad AMPK-DN before adipogenic differentiation. Then, cultures were induced to differentiate with TP or γ-T3 for 7 days. Adenoviral infection of Ad AMPK-DN was confirmed by an increase of total AMPK protein levels, with a decrease of phosphorylated AMPK protein levels. Infection of Ad AMPK-DN caused a slight reduction of adipogenesis in basal levels. The blockage of AMPK activation rescued the PPAR-γ protein in γ-T3-treated cultures comparable to TP control (Fig. 6A). However, inhibition of AMPK activation was only partially effective in restoring lipid-loaded morphology of adipocytes in γ-T3 treated cultures (Fig. 6B). Despite a significant

increase of PPAR-γ expression, mRNA levels of PLIN, a lipid droplet-coating protein of adipocytes, were not affected by AMPK inhibition (Fig. 6C). More intriguingly, inhibition of AMPK activation failed to dampen the γ-T3-mediated autophagosome formation and p62 degradation (Fig. 6A). These data suggest that γ-T3-induced a unique autophagy pathway that is independent to AMPK activation and plays a key role in opposing adipogenesis.

4 Discussion

The goal of this study was to investigate the effect of γ-T3 on new fat cell formation focusing on the signal modification during adipogenesis. We demonstrated definitively that γ-T3 specifically suppressed the early stage of adipogenesis and promoted apoptosis through pathways associated with AMPK and autophagy, with little impact on mature adipocytes (Fig. 4–6). To our knowledge, this study is the first report that γ-T3 induces AMPK and autophagy activation reducing adipogenesis in primary *h*ASCs, a physiologically more relevant adipocyte model to humans than 3T3L1 murine preadipocytes. Collectively, our work here suggests that suppression of adipogenic conversion by γ-T3 may constitute a new dietary strategy to manage hyperplastic obesity.

The seminal observation that γ-T3 plays an inhibitory role in adipogenesis was also provided by the 3T3L1 cell line [33]. In several aspects, our results from *h*ASCs are compatible with those from 3T3L1 cells. In both studies, γ-T3 and δ-T3 displayed stronger anti-adipogenic effects than α-T3, suggesting that the lack of a methyl group at position 5 (R1) of the chromanol ring may contribute to the inhibitory activity. The inhibitory activity may be due to generation of a bioactive metabolite of T3 by ω-oxidation [47], although it has not yet been identified. In addition, the active dose range to inhibit adipogenesis was similar in the two adipocyte models. γ-T3 inhibits approximately 80–90% of adipogenic gene expression in 3T3L1 cells at 0.024 ~2.4 μM [33]. Similarly, our data also showed that ~90% suppression of adipogenesis was achieved by treatment with 1 μM γ-T3 (Fig. 2, 3). Importantly, anti-adipogenic activity is limited to early-phase adipogenesis without affecting pre-existing adipocytes in both murine [33] and human adipocyte progenitor cells (Fig. 2C). Based on results from two different cell models of adipocytes, it is indicative that an adequate dose of γ-T3 for inhibition of adipogenesis is physiologically attainable by oral supplementation without causing dedifferentiation of mature adipocytes. One of the distinct metabolic differences between 3T3L1 cells and *h*ASCs with γ-T3 treatment arises from the insulin response. Uto-Kondo et al. concluded that the anti-adipogenic response of γ-T3 in 3T3L1 cells is due to the decreased-Akt phosphorylation upon insulin stimulation [33], which was not the case in *h*ASCs (Fig. 4A).

Our next signaling focus was AMPK and autophagy. Adipocyte differentiation is an anabolic process that is sensed by "nutritionally affluent" signals strictly coupled to energy storage demands. AMPK is regarded as a major energy-sensing regulator that activates a variety of catabolic processes and simultaneously prevents anabolic processes via inhibition of the mTOR pathway [48]. Although the direct roles of nutrient-sensing signaling in adipogenesis are not fully understood, it appears that adipogenesis is highly susceptible to the changes in the cellular energy status. Broad ranges of phytochemicals have been reported to suppress adipogenesis through the AMPK pathway in vitro and in vivo [29, 30, 38, 49, 50]. As we expected, an inverse relationship between the AMPK and mTOR pathways was observed in *h*ASCs, confirming a global growth-inhibitory action of *γ*-T3 during adipogenesis (Fig. 4B, C). In parallel to previous reports that AICAR, a pharmacological agonist of AMPK, almost completely blocks adipogenesis of 3T3L1 cells [49], we also found that AICAR was also effective in inhibiting adipogenesis in *h*ASCs (data not shown). The upstream mechanism by which *γ*-T3 induces AMPK activation is likely dependent on intracellular calcium activation. Our unpublished data showed that *γ*-T3 triggers upregulation of intracellular calcium levels (data not shown). Further studies for identification of upstream targets of AMPK activation will reveal the upstream signaling partners that synergistically act to antagonize adipogenesis. The underlying mechanism by which *γ*-T3 activates AMPK is currently being investigated to elucidate mechanistic details.

Autophagy is a lysosomal degradation pathway that degrades damaged or superfluous cell components for stress adaptation or survival [51–53]. Although there are remaining questions about whether adipogenesis is coupled to mitochondria-specific autophagy (mitophagy) or not, recent work has established that autophagy is required to fulfill the white adipocyte development in vivo and in vitro [26, 27]. In our study, we have demonstrated that autophagic degradation concurrently occurred at the same time as transcriptional activation of PPAR-*γ* in *h*ASCs (Fig. 5A, B). Surprisingly, we have demonstrated that *γ*-T3 increased autophagy even further than the normal adipogenic process. In addition, *γ*-T3- mediated autophagosomes seem to have a different composition based on decreased levels of beclin1 (Fig. 5C). Due to the limited knowledge of adipocyte autophagy and technical difficulties in distinguishing autophagic pathways (i.e. macroautophagy, mitophagy, and lipophagy), it is difficult to understand the precise molecular nature of *γ*-T3-mediated autophagy. Further studies are required to determine the physiological importance of *γ*-T3-mediated autophagy during adipogenesis by comparing autophagosome components. However, we assume that *γ*-T3-mediated autophagy is a process that is associated with subsequent Bcl-2/caspase 3 mediated apoptosis (Fig. 5D–F). Our results indicate that autophagy is a critical signaling checkpoint for determining whether mesenchymal

stem cells differentiate into adipocytes or undergo the alternative cell-death pathway based on the micro-environmental setting.

It has been documented that the mTOR/AMPK /autophagy axis is coordinately regulated by fuel availability via the molecular mediator Ulk1 phosphorylation in glucose-depleted situation [52, 54]. It did not seem to apply to the γ-T3 treatment in *h*ASCs: We failed to detect Ulk1 phosphorylation (Ser 317, data not shown); the blockage of AMPK activation was unable to inhibit γ-T3-mediated autophagy (Fig. 6A).Moreover, the rescue of PPAR-γ without normalization of autophagy was not effective in complete restoration of adipocyte morphology (Fig. 6B, C). Defective adipocyte morphology may be a result of, at least in part, low levels of PLIN that protects lipid droplets from cytosolic lipases. It has not been investigated whether γ-T3-induced autophagosome is engulfing lipids (lipophagy) or specific coactivators for PPAR-γ. Further research on understanding the molecular nature of γ-T3-induced autophagy is underway. Taken together, our data also lead us to conclude that γ-T3-mediated AMPK and autophagy activation are two independent mechanisms that synergistically inhibit the adipogenesis of *h*ASCs.

In conclusion, our study demonstrated that γ-T3 efficiently suppresses early adipogenic processes in *h*ASC through growth inhibitory signaling pathways including AMPK and autophagy activation. Although additional studies are required to determine the exact molecular nature, our study has provided a novel insight into an anti-adipogenic role of AMPK and autophagy activation by γ-T3.

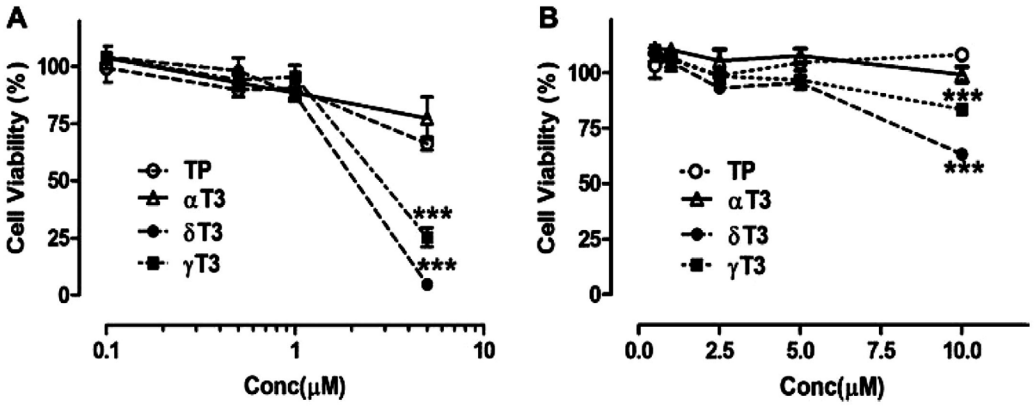

Figure 1. Effects of tocotrienols (T3) on cell viability in *h*ASCs. Cultures of *h*ASCs containing either undifferentiated **(A)** or differentiated **(B)** cells were treated with 0.1–10 μM tocopherol (TP, ○) or α-(Δ), δ-(●), and γ-(■) T3 for 24 h. XTT reagent was added 3 h before measurement of OD450. Data are expressed as a percentage of the vehicle control (DMSO). Each data point represents the mean ± SEM (n = 6). * $p < 0.05$; ** $p < 0.01$; *** $p < 0.001$ by one-way ANOVA.

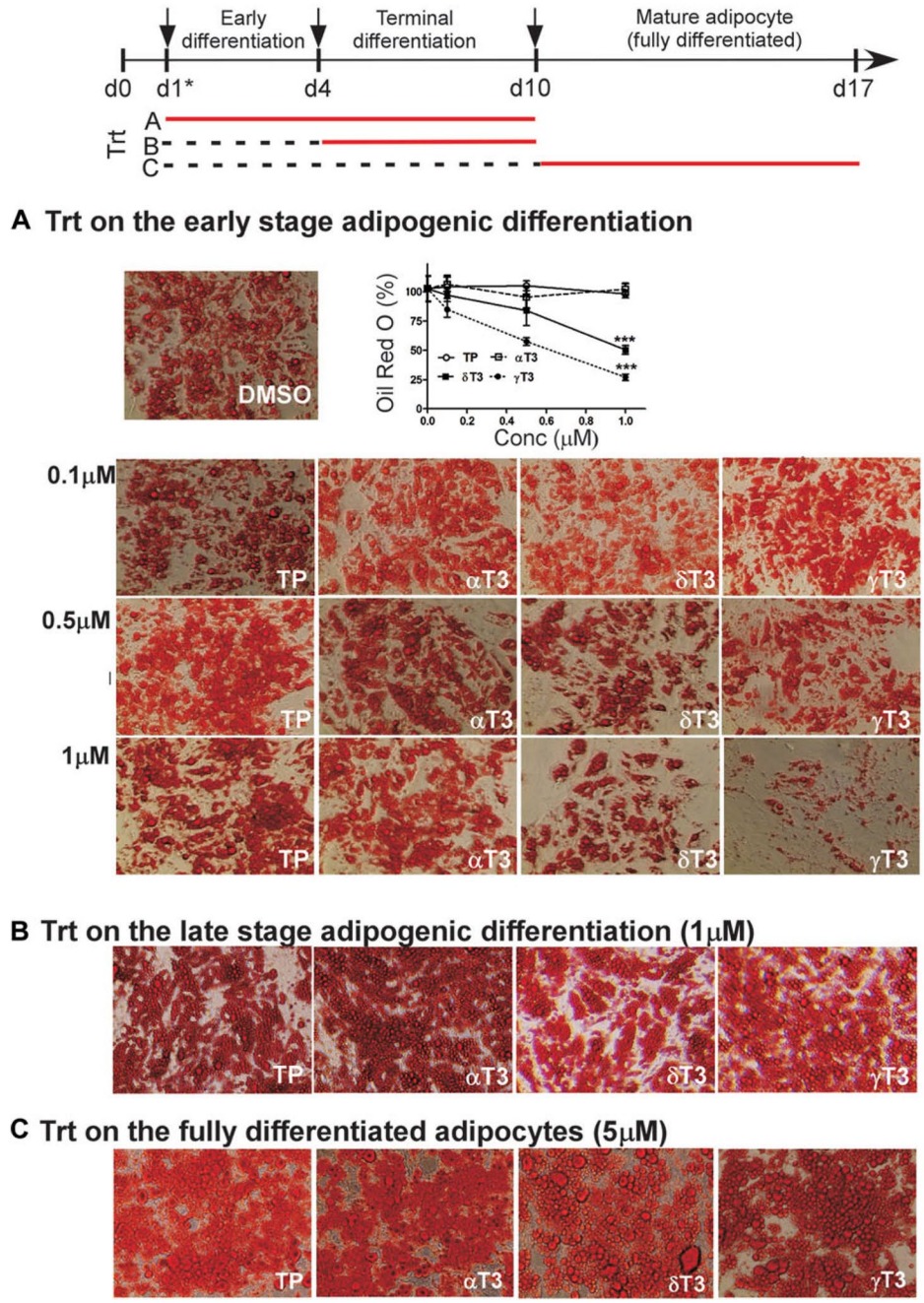

Figure 2. *γ*-, δ-T3s selectively suppress early-phase adipogenesis but not terminal differentiation. *h*ASCs were seeded at the day before differentiation (d0) and induced to differentiate the next day (d1*). TP, α-, δ-, and *γ*-T3s, or DMSO (vehicle control) were added at different phases of adipogenesis (shown in arrow). The effects of TP and T3 on early-stage adipogenesis (0.1–1 μM) **(A)**, late-stage adipogenesis (1 μM) **(B)**, or fully differentiated adipocytes (5 μM) **(C)** were examined. Red bars indicate the duration of T3 isomer treatment. Triglyceride accumulation was visualized by Oil red-O staining and representative images from three separate experiments are shown. Extracted staining was quantified (OD500 nm) and relative TG accumulation to the DMSO control was graphed in A. *** $p < 0.001$ by one-way ANOVA.

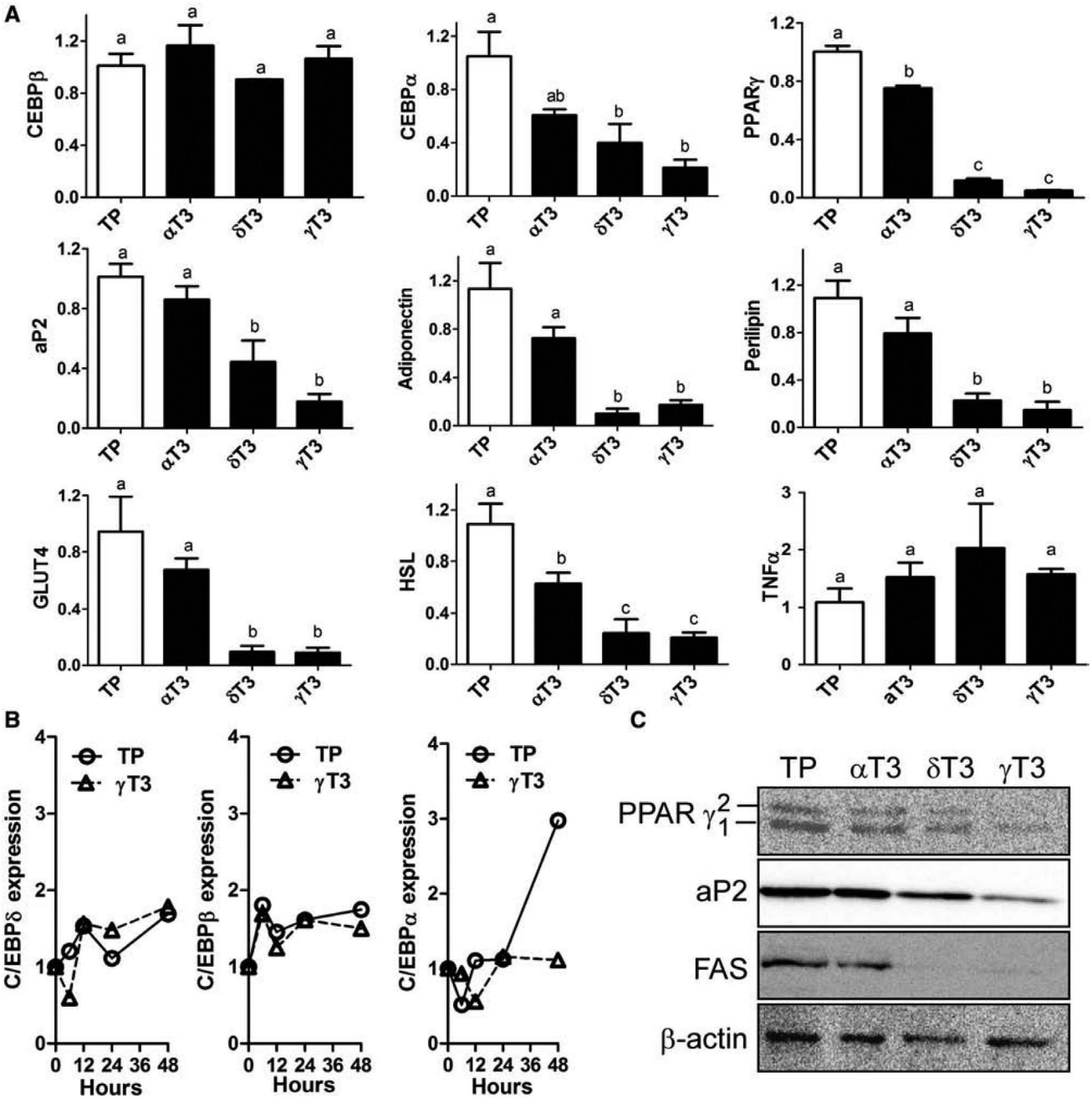

Figure 3. *γ*-, δ-T3s repress adipogenic gene and protein expression in *h*ASCs. Cultures of *h*ASCs were induced to differentiate in the presence of either 1 μM TP or α-, δ-, or *γ*-T3 for 10 days. **(A)** qPCR analysis for adipogenic gene expression of C/EBP-β, C/EBP-α, PPAR-*γ*, aP2, adiponectin, PLIN, glucose transporter 4, hormone-sensitive lipase, and TNF-α normalized by the average of two reference genes (36B4 and GAPDH), **(B)** Effects of *γ*-T3 (1 μM) on the dynamics of the adipogenic transcription factors C/EBP-δ, C/EBP-β, and C/EBP-α during early adipogenesis (0, 6, 12, 24, and 48 h). **(C)** Total cell extracts were immunoblotted for adipogenic protein expression of PPAR-*γ*, aP2, FAS. β-actin was used as a loading control. In A, data are expressed as the mean ± SEM from $n = 4$ samples of two separate experiments. Means not sharing a common superscript differ by one-way ANOVA ($p < 0.05$). In B, duplicate samples were pooled for qPCR analysis.

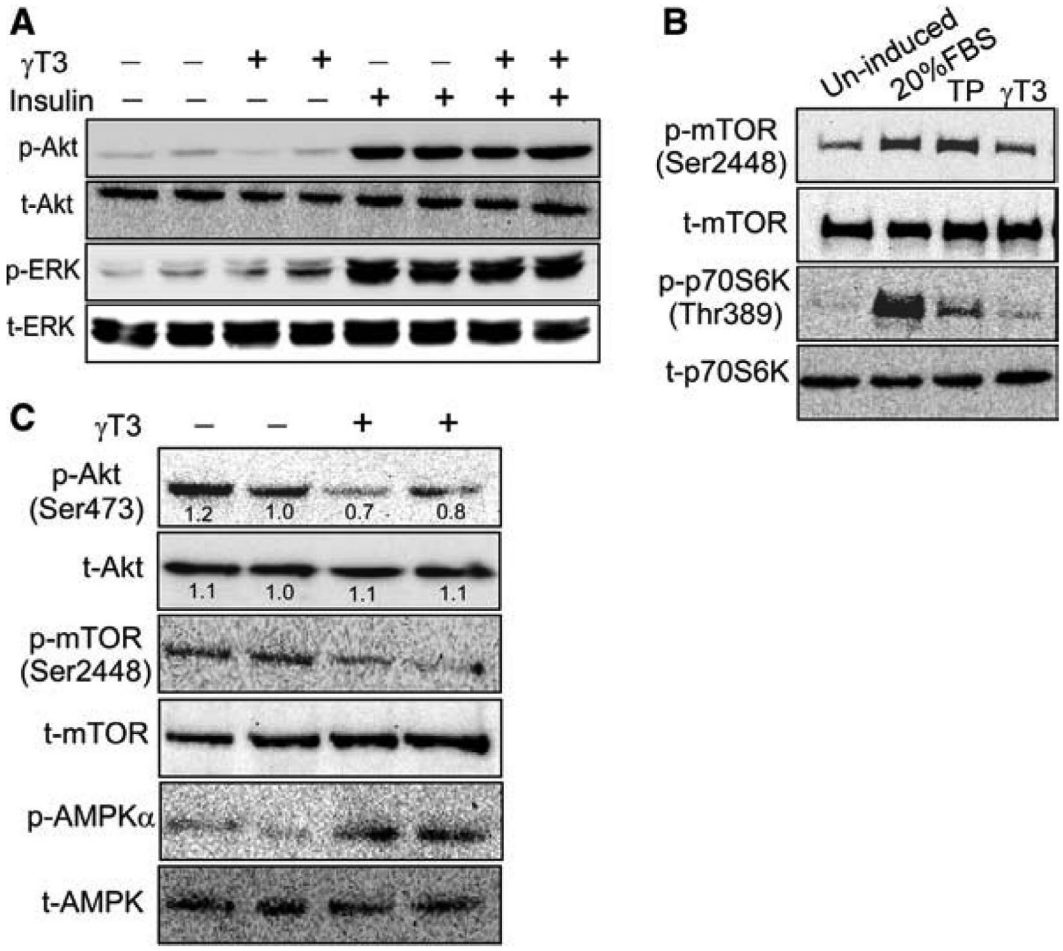

Figure 4. *γ*-T3 modulates nutrient-sensing pathways of the Akt/mTOR/AMPK axis. Cultures of *h*ASCs were differentiated for 6 days in the presence or absence (DMSO only) of *γ*-T3. **(A)** Cultures were stimulated with (+) or without (−) human insulin (100 nM) for 10 min. Total cell extracts were immunoblotted for phospho-specific or total antibodies targeting protein kinase B (Akt, ERK). **(B)** Cultures were treated with 1 μM TP, or *γ*-T3 for 3 h in serum-free media. Fetal bovine serum stimulation (20%) for 30 min was used as a positive control for mTOR activation. After treatment, total cell extracts were immunoblotted for total and phospho-specific mTOR and p70 S6 ribosomal protein kinase (p70S6K). (C) Cultures were treated for 3 h with (+) or without (−, DMSO only) 1 μM *γ*-T3. Total cell extracts were immunoblotted using phosphospecific or total antibodies for Akt, mTOR, and AMPK.

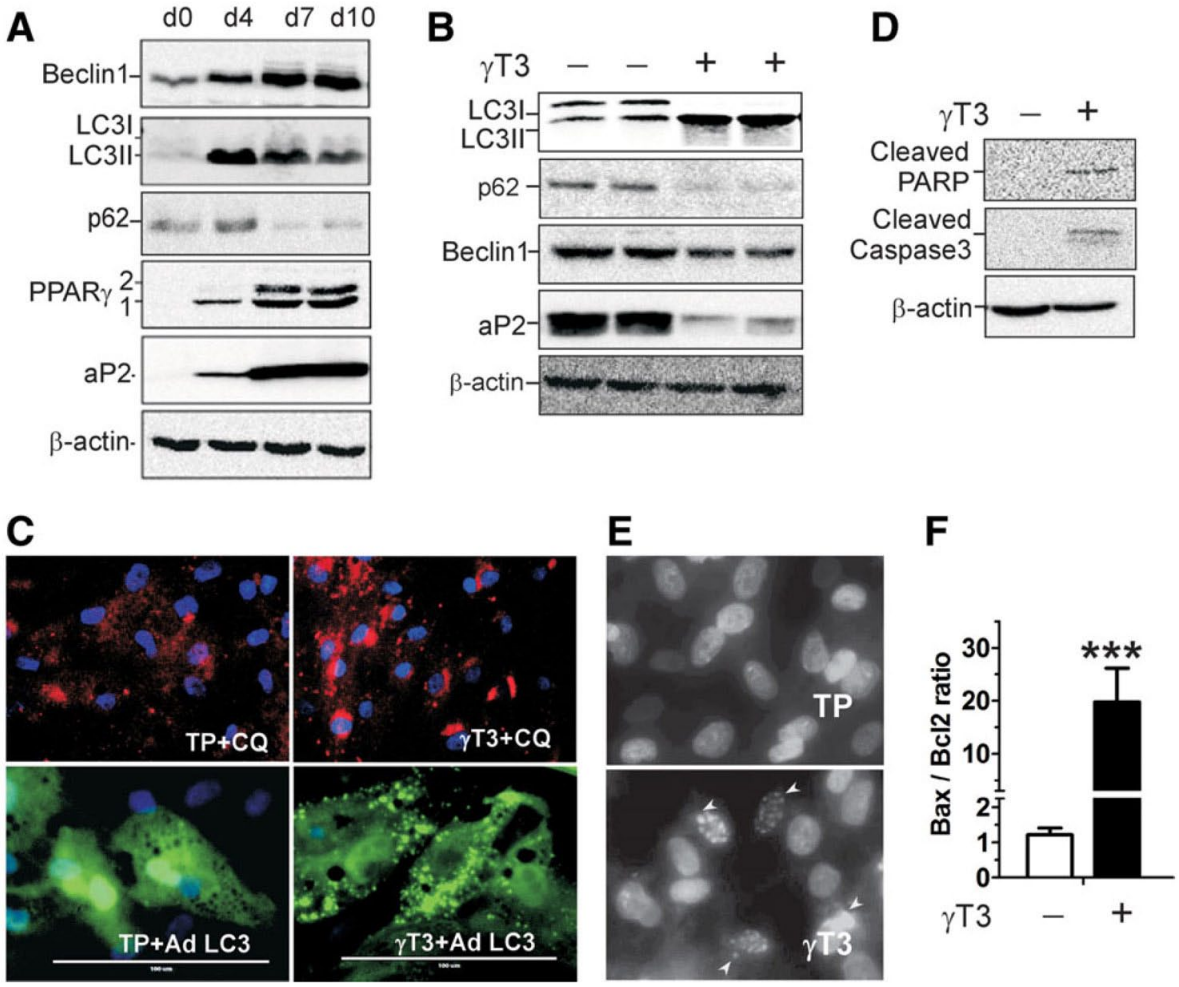

Figure 5. *γ*-T3 promotes autophagy. **(A)** Increase of beclin-1, autophagosome formation (LC3II), and p62 degradation during adipogenic differentiation in *h*ASCs. PPAR-*γ*, and aP2 were also shown as evidence for differentiation. **(B)** Western blot analysis of beclin-1, LC3, p62, and aP2 expression with or without *γ*-T3 for 7 days in differentiating *h*ASCs. **(C)** Immunostaining of LC3 in the presence and absence of *γ*-T3. CQ was added at the last 4 h before fixing the cells (upper panel). Autophagosome formation by *γ*-T3 was also confirmed by adenoviral infection of GFP-tagged Ad LC3 (lower panel). **(D)** Western blot analysis of cleaved-PARP and cleaved-caspase3. **(E)** Cultures grown in the presence or absence (DMSO only) of *γ*-T3 for 10 days were fixed and the nuclei were stained with DAPI. Arrows indicate condensed or fragmented nuclei. **(F)** The relative ratio of Bax and Bcl-2 gene expression at 10 days of adipogenic differentiation was obtained by qPCR. Representative images from three separate experiments with duplicated samples are shown in A and B. ***$p < 0.001$ by Student's *t*-test.

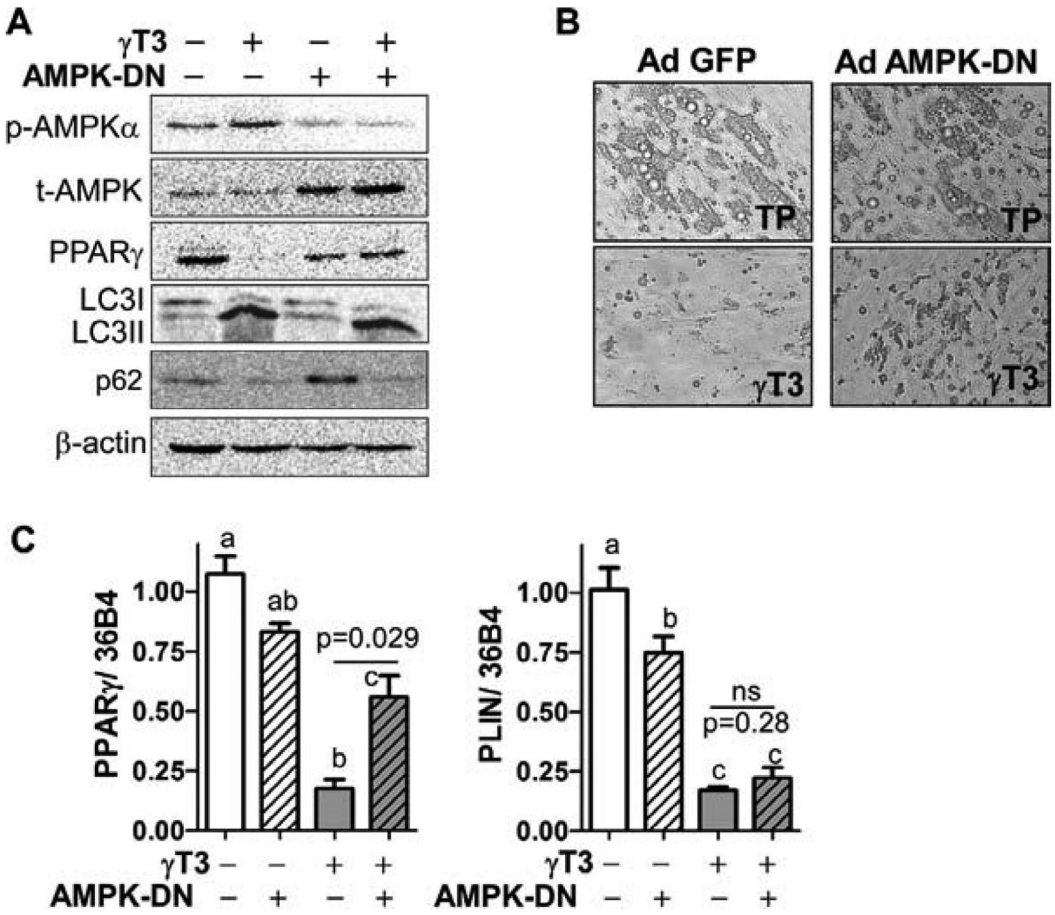

Figure 6. Inhibition of AMPK activation partially reverses the anti-adipogenic effects of *γ*-T3 in *h*ASCs. **(A)** Western blot analysis of phosphor-specific and total AMPK, PPAR-*γ*, and LC3 expression in the presence or absence of 1 μM *γ*-T3 treatment in Ad GFP or Ad AMPK-DN (Ad expressing DN AMPK) infected *h*ASCs. **(B)** Adenoviral overexpression of DN AMPK partially rescues adipocyte morphology. Phase-contrast images after 7 days of differentiation with either TP or *γ*-T3 in Ad GFP and Ad-AMPK-DN infected cultures. Results are representative of two independent experiments with triplicated samples. **(C)** PPAR-*γ* and PLIN mRNA expression in the presence or absence of 1 μM *γ*-T3 treatment in Ad GFP or Ad-AMPK-DN infected *h*ASCs. Results are normalized to Ad GFP infected cells, and are expressed as mean ± SEM of triplicate analyses. Values not sharing a common letter differ significantly by one-way ANOVA with Tukey's multiple comparison.

Acknowledgments — Supported by American Heart Association SDG grant (13SDG-14410043) to S.C. Isomers of palm tocotrienols were kindly supplied by W. H. Leong (Carotech, Inc., Edison, NJ). We gratefully acknowledge Meri Nantz (Food Science and Human Nutrition, University of Florida) and Dr. Vernon Rayner for editing the manuscript. The authors have declared no conflict of interest.

5 References

[1] Li, F., Tan, W., Kang, Z., Wong, C. W., Tocotrienol enriched palm oil prevents atherosclerosis through modulating the activities of peroxisome proliferators-activated receptors. *Atherosclerosis* 2010, *211*, 278–282.

[2] Das, S., Mukherjee, S., Lekli, I., Gurusamy, N. et al., Tocotrienols confer resistance to ischemia in hypercholesterolemic hearts: Insight with genomics. *Mol. Cell Biochem.* 2012, *360*, 35–45.

[3] Black, T. M., Wang, P., Maeda, N., Coleman, R. A., Palm tocotrienols protect ApoE +/− mice from diet-induced atheroma formation. *J. Nutr.* 2000, *130*, 2420–2426.

[4] Burdeos, G. C., Nakagawa, K., Kimura, F., Miyazawa, T., Tocotrienol attenuates triglyceride accumulation in HepG2 cells and F344 rats. *Lipids* 2012, 1–11.

[5] Zaiden, N., Yap, W. N., Ong, S., Xu, C. H. et al., Gamma delta tocotrienols reduce hepatic triglyceride synthesis and VLDL secretion. *J. Atheroscler. Thromb.* 2010, *17*, 1019–1032.

[6] Wong, W. Y., Poudyal, H., Ward, L. C., Brown, L., Tocotrienols reverse cardiovascular, metabolic and liver changes in high carbohydrate, high fat diet-fed rats. *Nutrients* 2012, *4*, 1527–1541.

[7] Fang, F., Kang, Z., Wong, C., Vitamin E tocotrienols improve insulin sensitivity through activating peroxisome proliferator gamma activated receptors. *Mol. Nutr. Food Res.* 2010, *54*, 345–352.

[8] Kaup, R. M., Khayyal, M. T., Verspohl, E. J., Antidiabetic effects of a standardized Egyptian rice bran extract. *Phytother. Res* 2013, *27*, 264–271.

[9] Jiang, Q., Rao, X., Kim, C. Y., Freiser, H. et al., Gamma-tocotrienol induces apoptosis and autophagy in prostate cancer cells by increasing intracellular dihydrosphingosine and dihydroceramide. *Int. J. Cancer* 2012, *130*, 685–693.

[10] Nesaretnam, K., Meganathan, P., Veerasenan, S. D., Selvaduray, K. R., Tocotrienols and breast cancer: The evidence to date. *Genes Nutr.* 2012, *7*, 3–9.

[11] Shin-Kang, S., Ramsauer, V. P., Lightner, J., Chakraborty, K. et al., Tocotrienols inhibit Akt and ERK activation and suppress pancreatic cancer cell proliferation by suppressing the ErbB2 pathway. *Free Radic. Biol. Med.* 2011, *51*, 1164–1174.

[12] Viola, V., Pilolli, F., Piroddi, M., Pierpaoli, E. et al., Why tocotrienols work better: Insights into the in vitro anti-cancer mechanism of vitamin E. *Genes Nutr.* 2012, *7*, 29–41.

[13] Kannappan, R., Gupta, S. C., Kim, J. H., Aggarwal, B. B., Tocotrienols fight cancer by targeting multiple cell signaling pathways. *Genes Nutr.* 2012, *7*, 43–52.

[14] Ahn, K. S., Sethi, G., Krishnan, K., Aggarwal, B. B., Gamma-tocotrienol inhibits nuclear factor-kappaB signaling pathway through inhibition of receptor-interacting protein and TAK1 leading to suppression of antiapoptotic gene products and potentiation of apoptosis. *J. Biol. Chem.* 2007, *282*, 809–820.

[15] Manu, K. A., Shanmugam, M. K., Ramachandran, L., Li, F. et al., First evidence that gamma-tocotrienol inhibits the growth of human gastric cancer and chemosensitizes it to capecitabine in a xenograft mouse model through the modulation of NF-kappaB pathway. *Clin. Cancer Res.* 2012, *18*, 2220–2229.

[16] Xu, W., Du, M., Zhao, Y., Wang, Q. et al., gamma-Tocotrienol inhibits cell viability through suppression of beta-catenin/Tcf signaling in human colon carcinoma HT-29 cells. *J. Nutr. Biochem.* 2012, *23*, 800–807.

[17] Wilankar, C., Sharma, D., Checker, R., Khan, N. M. et al., Role of immunoregulatory

transcription factors in differential immunomodulatory effects of tocotrienols. *Free Radic. Biol. Med.* 2011, *51*, 129–143.
[18] Rickmann, M., Vaquero, E. C., Malagelada, J. R., Molero, X., Tocotrienols induce apoptosis and autophagy in rat pancreatic stellate cells through the mitochondrial death pathway. *Gastroenterology* 2007, *132*, 2518–2532.
[19] Vaquero, E. C., Rickmann, M., Molero, X., Tocotrienols: Balancing the mitochondrial crosstalk between apoptosis and autophagy. *Autophagy* 2007, *3*, 652–654.
[20] Ogden, C. L., Carroll, M. D., Curtin, L. R., McDowell, M. A. et al., Prevalence of overweight and obesity in the United States, 1999–2004. *JAMA* 2006, *295*, 1549–1555.
[21] Sturm, R., Increases in morbid obesity in the USA: 2000–2005. *Public Health* 2007, *121*, 492–496.
[22] Spalding, K. L., Arner, E., Westermark, P. O., Bernard, S. et al., Dynamics of fat cell turnover in humans. *Nature* 2008, *453*, 783–787.
[23] Haberland, M., Carrer, M., Mokalled, M. H., Montgomery, R. L. et al., Redundant control of adipogenesis by histone deacetylases 1 and 2. *J. Biol. Chem.* 2010, *285*, 14663.
[24] Wright, W. S., Longo, K. A., Dolinsky, V. W., Gerin, I. et al., Wnt10b inhibits obesity in ob/ob and agouti mice. *Diabetes* 2007, *56*, 295–303.
[25] Ceddia, R. B., The role of AMP-activated protein kinase in regulating white adipose tissue metabolism. *Mol. Cell. Endocrinol.* 2012, *7*, 194–203.
[26] Baerga, R., Zhang, Y., Chen, P. H., Goldman, S. et al., Targeted deletion of autophagy-related 5 (atg5) impairs adipogenesis in a cellular model and in mice. *Autophagy* 2009, *5*, 1118–1130.
[27] Zhang, Y., Goldman, S., Baerga, R., Zhao, Y. et al., Adipose-specific deletion of autophagy-related gene 7 (atg7) in mice reveals a role in adipogenesis. *Proc. Natl. Acad. Sci. U.S.A.* 2009, *106*, 19860–19865.
[28] Ahn, J., Lee, H., Kim, S., Ha, T., Curcumin-induced suppression of adipogenic differentiation is accompanied by activation of Wnt/beta-catenin signaling. *Am. J. Physiol. Cell. Physiol.* 2010, *298*, C1510–C1516.
[29] Chen, Y. Y., Lee, M. H., Hsu, C. C., Wei, C. L. et al., Methyl cinnamate inhibits adipocyte differentiation via activation of the CaMKK2-AMPK pathway in 3T3-L1 preadipocytes. *J. Agric. Food Chem.* 2012, *60*, 955–963.
[30] Ono, M., Fujimori, K., Antiadipogenic effect of dietary apigenin through activation of AMPK in 3T3-L1 cells. *J. Agric. Food Chem.* 2011, *59*, 13346–13352.
[31] Dave, S., Kaur, N. J., Nanduri, R., Dkhar, H. K. et al., Inhibition of adipogenesis and induction of apoptosis and lipolysis by stem bromelain in 3T3-L1 adipocytes. *PLoS. One* 2012, *7*, e30831.
[32] Kim, H. K., Della-Fera, M. A., Lin, J., Baile, C. A., Docosahexaenoic acid inhibits adipocyte differentiation and induces apoptosis in 3T3-L1 preadipocytes. *J. Nutr.* 2006, *136*, 2965–2969.
[33] Uto-Kondo, H., Ohmori, R., Kiyose, C., Kishimoto, Y. et al., Tocotrienol suppresses adipocyte differentiation and Akt phosphorylation in 3T3-L1 preadipocytes. *J. Nutr.* 2009, *139*, 51–57.
[34] Cho, Y. C., Jefcoate, C. R., PPAR-gamma1 synthesis and adipogenesis in C3H10T1/2 cells depends on S-phase progression, but does not require mitotic clonal expansion. *J. Cell Biochem.* 2004, *91*, 336–353.
[35] Skurk, T., Hauner, H., Primary culture of human adipocyte precursor cells: Expansion and differentiation. *Methods Mol. Biol.* 2012, *806*, 215–226.
[36] Kim, J. S., Nitta, T., Mohuczy, D., O'Malley, K. A. et al., Impaired autophagy: A mechanism of mitochondrial dysfunction in anoxic rat hepatocytes. *Hepatology* 2008, *47*, 1725–1736.
[37] Wang, J. H., Ahn, I. S., Fischer, T. D., Byeon, J. I. et al., Autophagy suppresses age-dependent ischemia and reperfusion injury in livers of mice. *Gastroenterology* 2011, *141*, 2188–2199.

[38] Lee, J. W., Choe, S. S., Jang, H., Kim, J. et al., AMPK activation with glabridin ameliorates adiposity and lipid dysregulation in obesity. *J. Lipid Res.* 2012, *53*, 1277–1286.
[39] Chung, S., Brown, J. M., Sandberg, M. B., McIntosh, M., Trans-10,cis-12 CLA increases adipocyte lipolysis and alters lipid droplet-associated proteins: Role of mTOR and ERK signaling. *J. Lipid Res.* 2005, *46*, 885–895.
[40] Alers, S., Loffler, A. S., Wesselborg, S., Stork, B., Role of AMPK-mTOR-Ulk1/2 in the regulation of autophagy: Cross talk, shortcuts, and feedbacks. *Mol. Cell Biol.* 2012, *32*, 2–11.
[41] Goldman, S. J., Zhang, Y., Jin, S., Autophagic degradation of mitochondria in white adipose tissue differentiation. *Antioxid. Redox Signal.* 2011, *14*, 1971–1978.
[42] Singh, R., Cuervo, A. M., Autophagy in the cellular energetic balance. *Cell Metab.* 2011, *13*, 495–504.
[43] He, C., Klionsky, D. J., Regulation mechanisms and signaling pathways of autophagy. *Annu. Rev. Genet.* 2009, *43*, 67–93.
[44] Stipanuk, M. H., Macroautophagy and its role in nutrient homeostasis. *Nutr. Rev.* 2009, *67*, 677–689.
[45] Wang, R. C., Levine, B., Autophagy in cellular growth control. *FEBS Lett.* 2010, *584*, 1417–1426.
[46] Kroemer, G., Levine, B., Autophagic cell death: The story of a misnomer. *Nat. Rev. Mol. Cell. Biol.* 2008, *9*, 1004–1010.
[47] Sontag, T. J., Parker, R. S., Influence of major structural features of tocopherols and tocotrienols on their omegaoxidation by tocopherol-omega-hydroxylase. *J. Lipid Res.* 2007, *48*, 1090–1098.
[48] Howell, J. J., Manning, B. D., mTOR couples cellular nutrient sensing to organismal metabolic homeostasis. *Trends Endocrinol. Metab* 2011, *22*, 94–102.
[49] Lee, H., Kang, R., Bae, S., Yoon, Y., AICAR, an activator of AMPK, inhibits adipogenesis via the WNT/beta-catenin pathway in 3T3-L1 adipocytes. *Int. J. Mol. Med.* 2011, *28*, 65–71.
[50] Vingtdeux, V., Chandakkar, P., Zhao, H., Davies, P. et al., Small-molecule activators of AMP-activated protein kinase (AMPK), RSVA314 and RSVA405, inhibit adipogenesis. *Mol. Med.* 2011, *17*, 1022–1030.
[51] Egan, D. F., Shackelford, D. B., Mihaylova, M. M., Gelino, S. et al., Phosphorylation of ULK1 (hATG1) by AMP-activated protein kinase connects energy sensing to mitophagy. *Science* 2011, *331*, 456–461.
[52] Kim, J., Kundu, M., Viollet, B., Guan, K. L., AMPK and mTOR regulate autophagy through direct phosphorylation ofULK1. *Nat. Cell Biol.* 2011, *13*, 132–141.
[53] Zhao, M., Klionsky, D. J., AMPK-dependent phosphorylation of ULK1 induces autophagy. *Cell Metab.* 2011, *13*, 119–120.
[54] Egan, D., Kim, J., Shaw, R. J., Guan, K. L., The autophagy initiating kinase ULK1 is regulated via opposing phosphorylation by AMPK and mTOR. *Autophagy* 2011, *7*, 643–644.

Supporting Information

Supplement Table 1. Primer sequences for qPCR

Gene	Forward/Reverse	Sequence (5′-3’)
C/EBPδ	Forward	AGTTCTTGGGACATAGGAGCGCA
	Reverse	GTACCTTAGCTGCATCAACAGGAG
C/EBPβ	Forward	CGTGTGTACACGGGACTGAC
	Reverse	CAACAAGCCCGTAGGAACAT
C/EBPα	Forward	CCACGCCTGTCCTTAGAAAG
	Reverse	CCCTCCACCTTCATGTAGAAC
PPARγ	Forward	GAGCCCAAGTTTGAGTTTGC
	Reverse	CTGTGAGGACTCAGGGTGGT
aP2	Forward	ACTGGGCCAGGAATTTGACGAAGT
	Reverse	TCTCGTGGAAGTGACGCCTTTCAT
Adiponectin	Forward	TTGAGGCTGGGCCATCTCCT
	Reverse	AGCTCCCAGCAACAGCATCC
Perilipin	Forward	ACATTAAAGGGAAGAAGTTGAAGC
	Reverse	TTCTCCTGCTCAGGGAGGT
GLUT4	Forward	GCTACCTCTACATCATCCAGAATCTC
	Reverse	CCAGAAACATCGGCCCA
HSL	Forward	CTCAGTGTGCTCTCCAAGTG
	Reverse	CACCCAGGCGGAAGTCTC
TNFα	Forward	GGCAGTCAGATCATCTTCTCG
	Reverse	GGTTTGCTACAACATGGGCTA
Bax	Forward	TGGAGCTGCAGAGGATGATTG
	Reverse	GAAGTTGCCGTCAGAAAACATG
Bcl-2	Forward	TTGCTTTACGTGGCCTGTTTC
	Reverse	GAAGACCCTGAAGGACAGCCAT
GAPDH	Forward	GGCCTCCAAGGAGTAAGACC
	Reverse	AGGGGAGATTCAGTGTGGTG
36B4	Forward	GAAGGCTGTGGTGCTGATG
	Reverse	GTGAGGTCCTCCTTGGTGAA

Supplement Figure 1

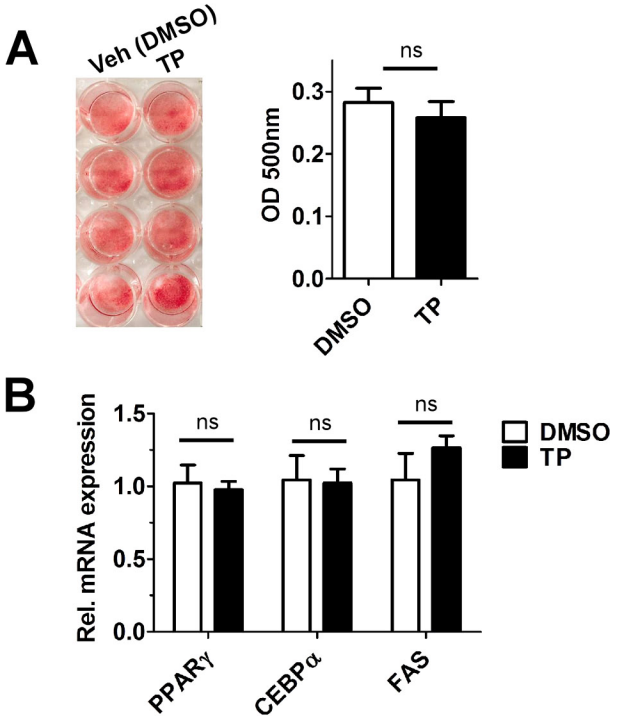

Supplement Figure 1. α-Tocoperol (TP) has no impact on triglyceride accumulation and adipogenic gene expression in *h*ASCs. To examine the effects of TP on adipogenesis, *h*ASCs were induced to differentiation with 1μM of TP or DMSO control for 7 days. **A**. TG accumulation by oil red-O staining (OD 500 nm). **B**. Adipogenic gene expression of PPARγ, C/EBPα and fatty acid synthase (FAS) by qPCR.